

Marquette University

e-Publications@Marquette

---

Chemistry Faculty Research and Publications

Chemistry, Department of

---

10-2018

## $\pi$ - $\pi$ stacking vs. C-H/ $\pi$ interaction: Excimer formation and charge resonance stabilization in van der Waals clusters of 9,9'-dimethylfluorene

Damian Kokkin  
*Marquette University*

Maxim Vadimovich Ivanov  
*Marquette University*

John Loman  
*Marquette University*

Sheng Cai  
*Marquette University*

Brandon Uhler  
*Marquette University*

*See next page for additional authors*

Follow this and additional works at: [https://epublications.marquette.edu/chem\\_fac](https://epublications.marquette.edu/chem_fac)

 Part of the [Chemistry Commons](#)

---

### Recommended Citation

Kokkin, Damian; Ivanov, Maxim Vadimovich; Loman, John; Cai, Sheng; Uhler, Brandon; Reilly, Neil; Rathore, Rajendra; and Reid, Scott A., " $\pi$ - $\pi$  stacking vs. C-H/ $\pi$  interaction: Excimer formation and charge resonance stabilization in van der Waals clusters of 9,9'-dimethylfluorene" (2018). *Chemistry Faculty Research and Publications*. 980.

[https://epublications.marquette.edu/chem\\_fac/980](https://epublications.marquette.edu/chem_fac/980)

---

**Authors**

Damian Kokkin, Maxim Vadimovich Ivanov, John Loman, Sheng Cai, Brandon Uhler, Neil Reilly, Rajendra Rathore, and Scott A. Reid

# $\pi$ - $\pi$ stacking vs. C-H/ $\pi$ interaction: Excimer formation and charge resonance stabilization in van der Waals clusters of 9,9'-dimethylfluorene

Cite as: J. Chem. Phys. **149**, 134314 (2018); <https://doi.org/10.1063/1.5044648>

Submitted: 14 June 2018 . Accepted: 20 September 2018 . Published Online: 05 October 2018

Damian Kokkin, Maxim Ivanov , John Loman, Jin-Zhe Cai, Brandon Uhler, Neil Reilly, Rajendra Rathore, and Scott A. Reid 



View Online



Export Citation



CrossMark

## ARTICLES YOU MAY BE INTERESTED IN

Davydov-type excitonic effects on the absorption spectra of parallel-stacked and herringbone aggregates of pentacene: Time-dependent density-functional theory and time-dependent density-functional tight binding

The Journal of Chemical Physics **149**, 134111 (2018); <https://doi.org/10.1063/1.5025624>

Fully anharmonic infrared cascade spectra of polycyclic aromatic hydrocarbons

The Journal of Chemical Physics **149**, 134302 (2018); <https://doi.org/10.1063/1.5038725>

Communication: Can excitation energies be obtained from orbital energies in a correlated orbital theory?

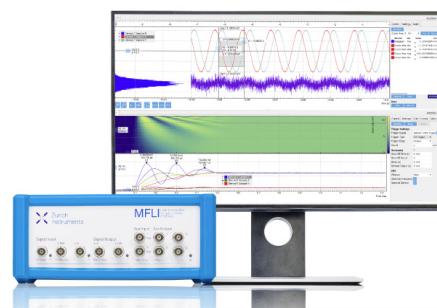
The Journal of Chemical Physics **149**, 131101 (2018); <https://doi.org/10.1063/1.5052442>

## Challenge us.

What are your needs for periodic  
signal detection?



Zurich  
Instruments



# $\pi$ - $\pi$ stacking vs. C-H/ $\pi$ interaction: Excimer formation and charge resonance stabilization in van der Waals clusters of 9,9'-dimethylfluorene

Damian Kokkin, Maxim Ivanov, John Loman, Jin-Zhe Cai, Brandon Uhler, Neil Reilly,<sup>a)</sup> Rajendra Rathore,<sup>b)</sup> and Scott A. Reid<sup>c)</sup>

*Department of Chemistry, Marquette University, Milwaukee, Wisconsin 53233, USA*

(Received 14 June 2018; accepted 20 September 2018; published online 5 October 2018)

Studies of exciton and hole stabilization in multichromophoric systems underpin our understanding of electron transfer and transport in materials and biomolecules. The simplest model systems are dimeric, and recently we compared the gas-phase spectroscopy and dynamics of van der Waals dimers of fluorene, 9-methylfluorene (MF), and 9,9'-dimethylfluorene (F1) to assess how sterically controlled facial encumbrance modulates the dynamics of excimer formation and charge resonance stabilization (CRS). Dimers of fluorene and MF show only excimer emission upon electronic excitation, and significant CRS as evidenced in a reduced ionization potential for the dimer relative the monomer. By contrast, the dimer of F1 shows no excimeric emission, rather structured emission from the locally excited state of a tilted (non  $\pi$ -stacked) dimer, evidencing the importance of C-H/ $\pi$  interactions and increased steric constraints that restrict a cofacial approach. In this work, we report our full results on van der Waals clusters of F1, using a combination of theory and experiments that include laser-induced fluorescence, mass-selected two-color resonant two-photon ionization spectroscopy, and two-color appearance potential measurements. We use the latter to derive the binding energies of the F1 dimer in ground, excited, and cation radical states. Our results are compared with van der Waals and covalently linked clusters of fluorene to assess both the relative strength of  $\pi$ -stacking and C-H/ $\pi$  interactions in polyaromatic assemblies and the role of  $\pi$ -stacking in excimer formation and CRS. *Published by AIP Publishing.* <https://doi.org/10.1063/1.5044648>

## I. INTRODUCTION

Multichromophoric assemblies have applications in areas from biochemistry to functional polymeric materials, and critically important in these assemblies are the fundamental processes of excimer and exciton formation and transport and charge resonance stabilization (CRS) or hole delocalization. For example, recent work has suggested that excimer formation is a trap state which hinders endothermic singlet fission.<sup>1</sup> Thus, studies of these processes in model compounds continue to be aggressively pursued, by experiment and theory.<sup>2-5</sup> For this purpose, we have utilized a set of model polyfluorenes covalently linked at the 9-position (denoted  $\mathbf{F}_n$ ;  $n = 1-6$ ),<sup>6-9</sup> which adopt a stacked (slipped) cofacial structure in the gas, liquid, and solid states.<sup>10</sup> Recently, excimer formation and CRS in the covalently linked  $\mathbf{F}_2$  dimer was compared with the van der Waals dimer of fluorene,  $(\mathbf{F})_2$ .<sup>11</sup> The measured ionization potentials (IPs) are identical; however, while both systems display solely excimeric emission and a lengthened fluorescence lifetime in comparison with the monomeric model, the excimeric state is stabilized (by

roughly  $\sim 30$  kJ/mol) in  $\mathbf{F}_2$  (Fig. S1 of the [supplementary material](#)). Supported by theory, this work demonstrated that optimal stabilization of an excimer requires a perfect sandwich-like geometry with maximal overlap, while geometrical requirements for hole stabilization in  $\pi$ -stacked aggregates are relaxed.<sup>11,12</sup>

The size evolution of charge resonance stabilization in the  $\mathbf{F}_n$  series, again compared with van der Waals clusters of fluorene [i.e.,  $(\mathbf{F})_n$  with  $n = 1-6$ ], was examined using mass-selected ion-yield (IY) and photoelectron spectroscopy.<sup>13</sup> Both systems show a  $1/n$  dependence of the gas-phase ionization potentials in the measured size range, reflecting the size evolution of hole delocalization.<sup>14</sup> Importantly, the  $1/n$  curves for  $(\mathbf{F})_n$  and  $\mathbf{F}_n$  fall essentially on the same line. Theoretical predictions using the benchmarked density functional theory (DFT) method reproduce this effect only for displaced,  $\pi$ -stacked van der Waals structures. Thus, this work emphasized the importance of  $\pi$ -stacking for efficient CRS as well as the relaxed geometrical requirement, i.e., not requiring a perfect sandwich-like configuration, for hole stabilization within  $\pi$ -stacked structures.

We have recently extended this comparison to the van der Waals dimer of  $\mathbf{F}_1$  (i.e., 9,9'-dimethylfluorene), in work that further demonstrated the importance of sandwich-like  $\pi$ -stacking for efficient excimer formation.<sup>15</sup> In contrast to  $(\mathbf{F})_2$  and (covalently linked)  $\mathbf{F}_2$ , the van der Waals dimer of  $\mathbf{F}_1$ , i.e.,  $(\mathbf{F}_1)_2$ , shows narrow features in its excitation

<sup>a)</sup>Present address: Department of Chemistry, University of Massachusetts, Boston, Massachusetts, USA

<sup>b)</sup>Deceased.

<sup>c)</sup>Author to whom correspondence should be addressed: [scott.reid@marquette.edu](mailto:scott.reid@marquette.edu)

spectrum, and no evidence of excimeric emission, as the measured fluorescence lifetime is similar to that of the monomer. Hole-burning spectroscopy confirmed that only one conformer contributed to the experimental spectrum,<sup>15</sup> and analysis of the torsional structure in dispersed fluorescence (DF) spectra showed that emission originated from the locally excited state of a tilted (non  $\pi$ -stacked) dimer, reflecting the increased importance of C–H/ $\pi$  interactions in the dimethyl substituted system, where increased steric hindrance prevents a co-facial approach and thus hinders the formation of sandwich-type structures.

In this article, we present our complete results of the  $(\mathbf{FI})_n$  clusters, which are compared with van der Waals and covalently linked clusters of fluorene. The structures of these clusters evidence the increased importance of C–H/ $\pi$  interactions—indeed, two-color appearance potential (2CAP) measurements of the ground state binding energy (BE) show that the non- $\pi$ -stacked  $\mathbf{FI}$  dimer,  $(\mathbf{FI})_2$ , is more strongly bound than  $\pi$ -stacked  $(\mathbf{F})_2$ . However, the influence of steric constraints enforced by methyl substitution has dramatic consequences for hole stabilization.<sup>15</sup> While IPs of  $(\mathbf{FI})_n$  clusters follow a linear trend with  $1/n$ , both the slope and intercept of the best-fit line evidence reduced CRS in comparison with van der Waals or covalently linked fluorene clusters. Consistent with this finding, the relative  $\mathbf{FI}$  dimer cation radical stabilization is decreased by some 50% in comparison with  $(\mathbf{F})_2$ . Our experimental results are compared with the predictions of previously benchmarked density functional theory (DFT) methods.

## II. METHODS AND MATERIALS

The experimental strategies used in these experiments have been described in detail.<sup>16,17</sup> Brief descriptions are provided here. Resonant 2-photon ionization (R2PI)<sup>18</sup> experiments were conducted in a linear 1 m time-of-flight mass spectrometer (TOFMS), equipped with a heated supersonic molecular beam source. Mass-selected excitation spectra were obtained using a one-color R2PI scheme (i.e., 1CR2PI), using the frequency doubled output of a Nd:YAG pumped dye laser. Ions were extracted and accelerated using a three-electrode stack, and they flew a distance of 1 m prior to striking a dual chevron microchannel plate detector. The detector signal was amplified, viewed, and recorded using a 100 Ms/s digital storage oscilloscope. Figure S2 of the [supplementary material](#) shows a mass spectrum under conditions optimized for cluster formation;  $(\mathbf{FI})_n$  clusters up to  $n = 11$  are observed.

Ion yield (IY) and two-color appearance potential (2CAP) measurements employed two-color excitation, where a second tunable frequency doubled dye laser system was introduced for ionization, with the timing of the two lasers controlled by a digital pulse/delay generator (BNC Nucleonics). Spectra were obtained by monitoring signal in the dimer (IY) or monomer (2CAP) mass channel while scanning the ionizing laser; typically 20 laser shots were averaged at each wavelength. Laser induced fluorescence (LIF) and dispersed fluorescence (DF) measurements were carried out in a separate chamber optimized for fluorescence, equipped with an identical heated supersonic molecular beam source.

To support our experimental findings, electronic structure calculations were performed using density functional theory (DFT) in the Gaussian 09 software package.<sup>19</sup> In earlier studies,<sup>11,20</sup> it has been found that accurate ground state energies of  $\pi$ -stacked dimers could be obtained using a simple PBE0 density functional<sup>21,22</sup> augmented with the D3 version of Grimme's dispersion term,<sup>23</sup> at a fraction of the cost of more sophisticated methods. However, an accurate description of the cation radical state is often a challenge for DFT methods due to the self-interaction error.<sup>24</sup> In our earlier study of the fluorene dimer,<sup>25</sup> we have shown that the CAM-B3LYP-D3 method provides a balanced description of the experimental binding energies at neutral, excited, and cation radical states,<sup>25</sup> while a calibrated<sup>26–28</sup> B1LYP<sup>29</sup> functional with 40% of Hartree Fock exchange (B1LYP-40) showed the best performance in reproducing binding energies of the cation radical state. Thus, all calculations of  $(\mathbf{FI})_2$  were performed using the PBE0-D3, CAM-B3LYP-D3, and B1LYP-40 methods with a cc-pVDZ basis set.<sup>30,31</sup> Binding energies of  $(\mathbf{FI})_2$  were corrected for zero point energies and basis set superposition error using the counterpoise method. To probe the potential energy surfaces (PESs) of  $(\mathbf{FI})_3$  and  $(\mathbf{FI})_4$  clusters, we performed molecular dynamics simulations with subsequent geometry optimizations using DFT; see the [supplementary material](#) for details.

## III. RESULTS AND DISCUSSION

To investigate the role of  $\pi$ -stacking on CRS, we initially consider the binding energies of the  $\mathbf{FI}$  van der Waals dimer,  $(\mathbf{FI})_2$ , contrasted with recent measurements for the fluorene dimer,  $(\mathbf{F})_2$ ,<sup>25</sup> which is  $\pi$ -stacked in ground, excited, and cation radical states. Prior hole-burning studies of  $(\mathbf{FI})_2$  suggest the presence of a single conformer, as noted above;<sup>15</sup> this is supported by new dispersed fluorescence (DF) spectra (Fig. S3 of the [supplementary material](#)) which show that excitation of the prominent features above the putative  $S_1$  origin gives rise to pronounced torsional activity in the DF spectra, suggesting that these transitions are associated with torsional excitation in the excited state.

Figure 1 displays relevant thermochemical cycles linking energy ladders of the  $\mathbf{FI}$  monomer and dimer,<sup>32</sup> with values derived from experimental R2PI measurements. We determined the binding energy in the ground ( $S_0$ ) state using the 2CAP method,<sup>25,32,33</sup> illustrated in Fig. 2(a). Here the ionizing photon is scanned above the dimer ionization potential, and the dimer breakdown energy is measured by monitoring fragmentation into the monomer mass channel. As shown, this energy equals the sum of the adiabatic monomer IP and ground  $S_0$  state dimer binding energy. It is important to emphasize that the 2CAP method, which has been previously used to derive binding energies for a range of non-covalent clusters,<sup>32</sup> provides only an upper limit to the true binding energy.<sup>25,32,33</sup>

Considering further the thermochemical cycle shown in Fig. 1, we emphasize that the determination of the ground state binding energy relies on the determination of the adiabatic ionization energy (AIE) of the *monomer*, for which ion yield (IY) spectra should provide a reliable estimate. Thus, while

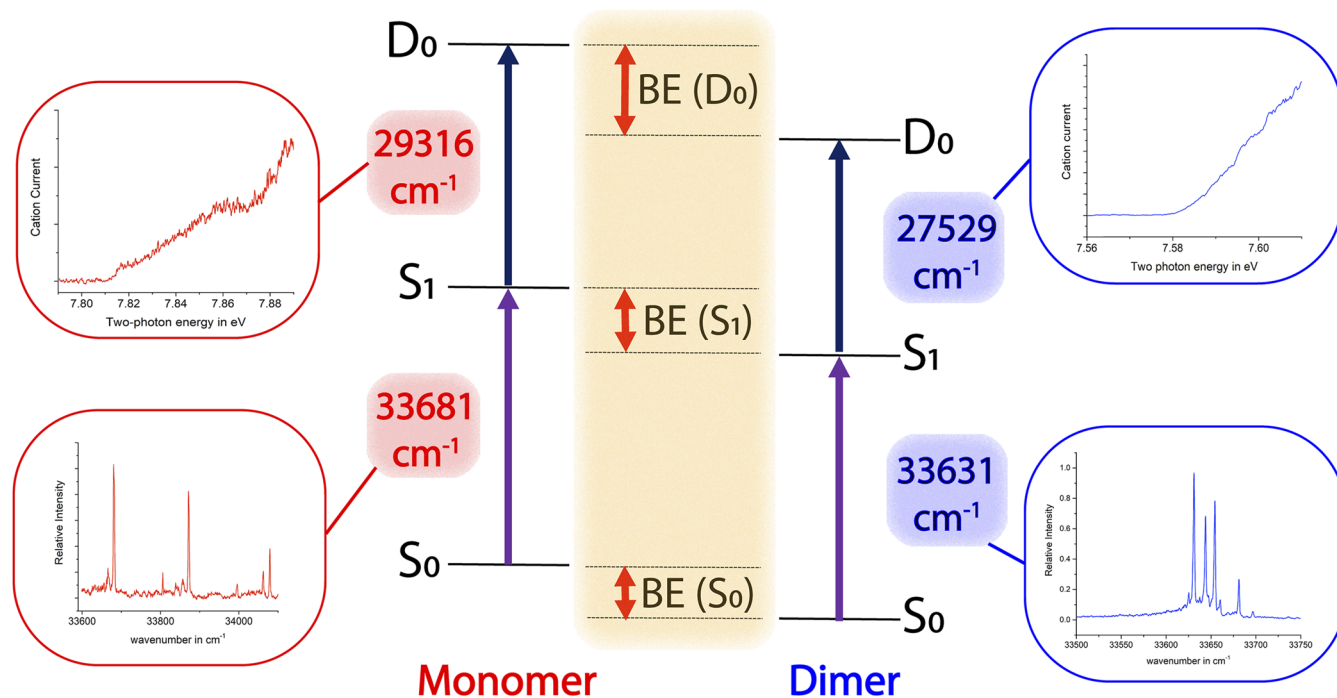


FIG. 1. Thermochemical cycle for determining binding energies in the  $S_0$ ,  $S_1$ , and  $D_0$  states of the F1 dimer. The values in each ladder have been determined from resonant two-photon ionization measurements, as described originally in Ref. 14.

still an upper limit, the 2CAP value of the ground state binding energy can be expected to closely approximate the true value. Then, application of the thermochemical cycle to determine the binding energy in  $S_1$  relies on the ability to determine the true electronic origins of the monomer and dimer, which here are determined to spectroscopic accuracy and their values thus not in doubt. Finally, determination of the binding energy in  $D_0$  (i.e., for the cation radical) relies on determination of AIE of the dimer, for which there is more potential ambiguity, due to the possibility of larger changes in geometry. However, here the IY curve of the dimer (Fig. 1) also displays a sharp threshold, suggesting that in this system the 2CAP method should provide upper limits that are close to the true values. An expanded view of the ion yield onset for monomer and dimer is shown in Fig. S4 in the [supplementary material](#).

The measured 2CAP profile of  $(\mathbf{F1})_2$  is shown in Fig. 2(b), with the energy axis defined relative to the ionization potential

of the monomer. A clear onset is observed, with analysis yielding an upper limit to the  $S_0$  binding energy (BE) of 0.457(70) eV. Somewhat surprisingly, the derived upper limit of the BE is larger than that of the fluorene dimer, evidencing the similar strength of  $\pi$ - $\pi$  and C-H/ $\pi$  forces.

Using the thermochemical cycles displayed in Fig. 1, we can readily estimate upper limits to the binding energies of  $(\mathbf{F1})_2$  in the  $S_1$  and  $D_0$  states, which are given in Table I. As expected, the upper limit to the binding energy in the  $S_1$  state is similar to that in  $S_0$ , as the origin-dominated spectrum evidences little geometry change in the vertical excitation. However, the binding energy in  $D_0$  is increased by some 50%. Again, given the sharp onsets in the ion yield curves, Fig. S4, we expect that these upper limits are in fact close to the true values.

Theoretical predictions for the  $(\mathbf{F1})_2$  binding energies are provided in Table I. In our benchmark study of  $(\mathbf{F})_2$ ,<sup>25</sup>

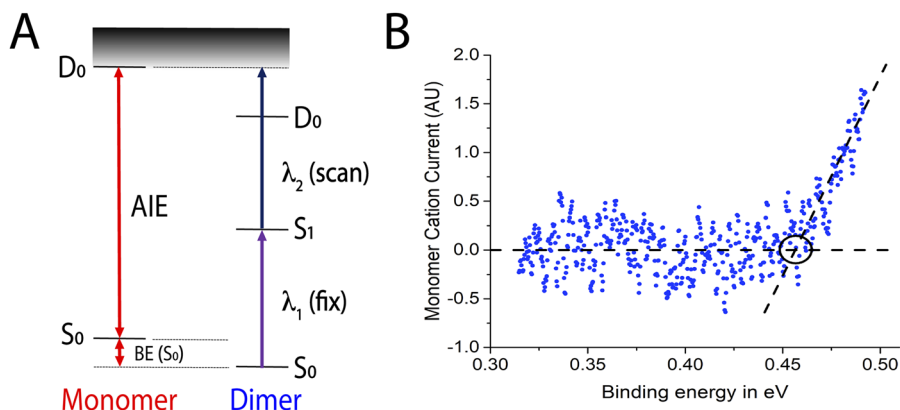


FIG. 2. (a) Schematic of the two-color appearance potential (2CAP) method. (b) 2CAP measurement of the F1 dimer, with energy given relative to the monomer AIE. The intersection of the two lines (circled) marks the binding energy.

TABLE I. Experimental and computed binding energies for the **F1** dimer, (**F1**)<sub>2</sub>. All DFT binding energies were corrected for zero-point energy and basis set superposition error using the counterpoise method.

Method	Structure <sup>a</sup>	Binding energy (kJ/mol)		
		S <sub>0</sub>	S <sub>1</sub>	D <sub>0</sub>
Experiment (2CAP) <sup>b</sup>		<44.1 ± 6.8	<44.7 ± 6.8	<66.1 ± 6.9
CAM-B3LYP-D3/cc-pVDZ	A	35.1	41.8	56.9
	B	29.5	37.3	54.5
	C	25.2	43.0	72.9
B1LYP40-D3/cc-pVDZ <sup>c</sup>	A	27.3	35.3	55.9
	B	23.3	31.6	51.3
	C	18.0	36.2	68.4
PBE0-D3/cc-pVDZ	A	39.4	58.9	79.0
	B	32.5	54.9	72.0
	C	29.9	65.8	93.6

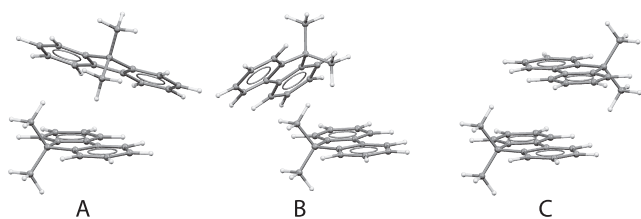
<sup>a</sup>A = tilted, B = one is flipped, C = displaced sandwich. See Scheme 1 and Ref. 14 for details.

<sup>b</sup>Upper limits, one standard error in parentheses.

<sup>c</sup>Dispersion parameters from CAM-B3LYP-D3 method were employed.

we showed that the CAM-B3LYP-D3 method best reproduced the experimental binding energy upper limits across ground (S<sub>0</sub>), excited (S<sub>1</sub>), and cation radical (D<sub>0</sub>) states, while the benchmarked B1LYP40–D3 method provided an accurate description of the cation radical state. By contrast, the PBE0–D3 method well reproduced the binding in S<sub>0</sub>, but severely overestimated the binding in excited and cation radical states. Table I gives predicted binding energies using these three methods for three different (**F1**)<sub>2</sub> structures identified earlier, which are reproduced in Scheme 1.<sup>15</sup> The measured ground (S<sub>0</sub>) state binding energy (upper limit) is most consistent with the values calculated using CAM-B3LYP-D3 or PBE0–D3 for the global minimum structure A, which is not  $\pi$ -stacked. By contrast, the CAM-B3LYP-D3 and B1LYP40–D3 calculations indicate that the derived binding energy (upper limit) of the cation radical state is most consistent with displaced  $\pi$ -stacked structure C (Scheme 1). This discussion, of course, assumes that the derived experimental upper limits are in fact close to the true values, a point elaborated above.

It is known that the fluorene dimer, upon excitation, rapidly rearranges from the ground state parallel orthogonal structure to a sandwich-like  $\pi$ -stacked excimeric structure, and ionization occurs then from the excimer well. Similarly, (**F1**)<sub>2</sub> may eventually rearrange to the frustrated excimer structure C upon electronic excitation (or ionization), as our experimental D<sub>0</sub> binding energy is consistent with that of structure C. Strikingly, calculations predict that the additional stabilization of

SCHEME 1. Relevant structures of (**F1**)<sub>2</sub>. See Ref. 14 for details.

the displaced,  $\pi$ -stacked structure C relative to structures A and B in the S<sub>1</sub> state is quite minimal, reflecting the steric hindrance imposed by 9,9' methyl substitution, which prevents formation of a true sandwich like geometry needed for efficient excimer stabilization.<sup>15</sup> However, the differential stabilization of  $\pi$ -stacked structure C is pronounced in the D<sub>0</sub> state, consistent with our prior findings of a relaxed geometrical constraint for efficient charge resonance stabilization.

To further probe CRS in this system, Fig. 3 displays excitation spectra (a), ion yield spectra (b), and ionization potentials (c), plotted vs. 1/*n*, for (**F1**)<sub>*n*</sub> clusters with *n* = 1–4, obtained using two-color resonant two-photon ionization spectroscopy (2CR2PI) methods. Comparing the excitation spectra to those of fluorene clusters,<sup>13</sup> the smaller clusters display sharper structures and smaller red-shifts from the monomer origin. With increasing size, the spectra continue to red-shift and fill in, exhibiting for (**F1**)<sub>4</sub> and higher clusters a very broad and congested profile, shown in R2PI spectra of clusters with *n* = 4–7, Fig. S5 in the [supplementary material](#). This likely evidences the presence of multiple conformers with similar energies. To examine the structural evolution with size, we carried out a computational analysis of the PES of the trimer (**F1**)<sub>3</sub> and tetramer (**F1**)<sub>4</sub>. In this analysis, molecular dynamics simulations followed by subsequent geometry optimizations using DFT showed that the relative energies of eight representative (**F1**)<sub>3</sub> structures lie in the 0–30 kJ/mol range. Interestingly, the single (displaced)  $\pi$ -stacked conformation displays the largest energy among all conformations, yet its ionization potential is the lowest, consistent with our previous data on fluorene clusters (**F**)<sub>*n*</sub>.<sup>13</sup> The clusters of (**F1**)<sub>4</sub> shown in Fig. S6 in the [supplementary material](#) can be taken as representative examples of the structures of higher order clusters, given the similarity in R2PI spectra for clusters with *n* ≥ 4 (Fig. S4). In contrast to the possible structures of fluorene clusters (**F**)<sub>*n*</sub>, which could be classified into three categories ( $\pi$ -stacked, C–H/ $\pi$ -stabilized, or hybrid), the (**F1**)<sub>3</sub> and (**F1**)<sub>4</sub> structures mainly display hybrid configurations stabilized by both  $\pi$ -stacking and

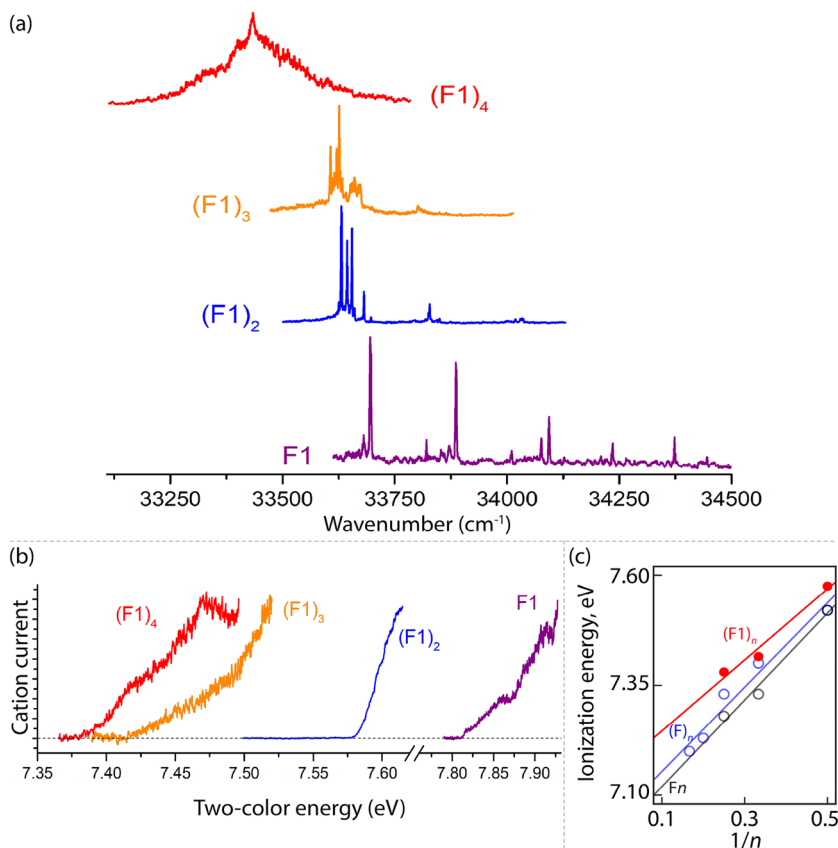


FIG. 3. (a) 2-color Resonant 2-photon Ionization (2CR2PI) spectra of van der Waals clusters of F1. (b) Ion yield spectra. (c) Ionization potentials, plotted vs.  $1/n$ .

C–H/ $\pi$  interactions (see Figs. S5 and S6 in the [supplementary material](#)).

The ionization thresholds, Fig. 3(b), of the smaller  $(\mathbf{F1})_n$  clusters display a trend of red-shift relative to the monomer, with the relative magnitude of the red-shift from one cluster to the next decreasing with increasing cluster size, Fig. 3(c). Excluding the monomer, the trend with cluster size indeed follows an approximate  $1/n$  dependence, as also observed for fluorene van der Waals clusters  $(\mathbf{F})_n$  and the covalent  $\mathbf{Fn}$  series. Indeed, as discussed above, the values for  $(\mathbf{F})_n$  and the covalent  $\mathbf{Fn}$  series fall on the same line, of slope 0.96 and intercept 7.06. Calculations reproduce this trend only for displaced  $\pi$ -stacked van der Waals clusters, as non- $\pi$ -stacked structures display uniformly higher IPs.<sup>13</sup> In this vein, we note that values of  $(\mathbf{F1})_n$  fall of a line of smaller slope (0.81) and larger intercept (7.17), Fig. 3(c), evidencing reduced CRS in the  $(\mathbf{F1})_n$  series. This is consistent with the dimer binding energy measurement discussed above.

These results, together with prior studies of fluorene van der Waals,  $(\mathbf{F})_n$ , and covalently linked,  $\mathbf{Fn}$ , clusters, paint a consistent picture of excimer formation and charge resonance stabilization in multichromophoric  $\pi$ -stacked assemblies. Excimer formation, absent in the  $(\mathbf{F1})_n$  series but dominant for  $(\mathbf{F})_n$  and  $\mathbf{Fn}$ , requires a perfect sandwich-like geometry for optimal electronic communication and orbital overlap. We have previously shown that the diminishing energetic gain from delocalization, which quickly saturates beyond two units in larger  $\mathbf{Fn}$ , leads to a localization of the exciton to a dimer subunit for all  $n$ .<sup>34</sup> On the other hand, charge resonance stabilization shows more extended delocalization,

following a  $1/n$  trend. The similarity in hole delocalization for displaced stacked van der Waals,  $(\mathbf{F})_n$ , and covalently linked,  $\mathbf{Fn}$ , clusters reflects the relaxed geometrical requirements for CRS in these assemblies. Simply stated, CRS does not require perfect sandwich like geometries yet is favored by  $\pi$ -stacked arrangements, and steric restrictions such as those found in the  $(\mathbf{F1})_n$  series further diminish its efficacy.

#### IV. CONCLUSIONS

In this work, we have examined the gas-phase spectroscopy and dynamics of van der Waals clusters of 9,9'-dimethylfluorene ( $\mathbf{F1}$ ) to assess the influence of sterically influenced facial encumbrance on the dynamics of excimer formation and charge resonance stabilization (CRS). This work has utilized a combination of theory and experiments that include laser-induced fluorescence (LIF), mass-selected two-color resonant two-photon ionization spectroscopy (2CR2PI), and two-color appearance potential (2CAP) measurements. We use the latter to derive the binding energy of  $(\mathbf{F1})_2$  in ground, excited, and cation radical states. The experimental ground state binding energy is in agreement with calculations for the global minimum energy structure, a tilted non- $\pi$ -stacked structure—surprisingly, this dimer is slightly more strongly bound than the  $\pi$ -stacked fluorene dimer, reflecting the similar strength of  $\pi$ - $\pi$  and C–H/ $\pi$  interactions.

In contrast to fluorene van der Waals,  $(\mathbf{F})_n$ , and covalently linked,  $\mathbf{Fn}$ , clusters, no excimer emission is observed in the  $(\mathbf{F1})_n$  series. This is consistent with our prior finding that

excimer formation requires a perfect sandwich-like geometry of two aromatic chromophores. In contrast to the possible structures of fluorene clusters ( $\mathbf{F}$ ) $_n$ , which can be classified into three categories ( $\pi$ -stacked, C–H/ $\pi$ -stabilized or hybrid), our calculations show that the ( $\mathbf{FI}$ ) $_n$  structures mainly display hybrid configurations stabilized by both  $\pi$ -stacking and C–H/ $\pi$  interactions. Interestingly, charge resonance stabilization follows a  $1/n$  trend for all three assemblies, although we find that CRS is favored by  $\pi$ -stacked arrangements, with the efficiency of CRS is diminished in the ( $\mathbf{FI}$ ) $_n$  series.

## SUPPLEMENTARY MATERIAL

See [supplementary material](#) for seven figures of additional experimental and computational data.

## ACKNOWLEDGMENTS

Support by the National Science Foundation (Grant No. CHE-1508677) is acknowledged. The calculations were performed on the high-performance computing cluster Pèrè at Marquette University funded by NSF Award Nos. OCI-0923037 and CBET-0521602 and the Extreme Science and Engineering Discovery Environment (XSEDE) funded by NSF (No. TG-CHE130101).

<sup>1</sup>C. B. Dover, J. K. Gallaher, L. Frazer, P. C. Tapping, A. J. Petty, M. J. Crossley, J. E. Anthony, T. W. Kee, and T. W. Schmidt, *Nat. Chem.* **10**(3), 305–310 (2018).

<sup>2</sup>J. C. Johnson, A. J. Nozik, and J. Michl, *Acc. Chem. Res.* **46**(6), 1290–1299 (2013).

<sup>3</sup>P. Ottiger, H. Koppel, and S. Leutwyler, *Chem. Sci.* **6**(11), 6059–6068 (2015).

<sup>4</sup>J. C. Johnson, A. Akdag, M. Zamadar, X. D. Chen, A. F. Schwerin, I. Paci, M. B. Smith, Z. Havlas, J. R. Miller, M. A. Ratner, A. J. Nozik, and J. Michl, *J. Phys. Chem. B* **117**(16), 4680–4695 (2013).

<sup>5</sup>A. A. Voityuk, *J. Phys. Chem. C* **114**(47), 20236–20239 (2010).

<sup>6</sup>R. Rathore, S. H. Abdelwahed, and I. A. Guzei, *J. Am. Chem. Soc.* **125**(29), 8712–8713 (2003).

<sup>7</sup>R. Rathore, V. J. Chebny, and S. H. Abdelwahed, *J. Am. Chem. Soc.* **127**(22), 8012–8013 (2005).

<sup>8</sup>R. Rathore, S. H. Abdelwahed, M. K. Kiesewetter, R. C. Reiter, and C. D. Stevenson, *J. Phys. Chem. B* **110**(4), 1536–1540 (2006).

<sup>9</sup>V. J. Chebny and R. Rathore, *J. Am. Chem. Soc.* **129**(27), 8458–8465 (2007).

<sup>10</sup>J. Vura-Weis, S. H. Abdelwahed, R. Shukla, R. Rathore, M. A. Ratner, and M. R. Wasielewski, *Science* **328**(5985), 1547–1550 (2010).

<sup>11</sup>N. Reilly, M. Ivanov, B. Uhler, M. Talipov, R. Rathore, and S. A. Reid, *J. Phys. Chem. Lett.* **7**(15), 3042–3045 (2016).

<sup>12</sup>D. A. Wang, M. V. Ivanov, D. Kokkin, J. Loman, J. Z. Cai, S. A. Reid, and R. Rathore, *Angew. Chem., Int. Ed.* **57**(27), 8189–8193 (2018).

<sup>13</sup>M. V. Ivanov, N. Reilly, B. Uhler, D. Kokkin, R. Rathore, and S. A. Reid, *J. Phys. Chem. Lett.* **8**(21), 5272–5276 (2017).

<sup>14</sup>M. V. Ivanov, M. R. Talipov, A. Boddada, S. H. Abdelwahed, and R. Rathore, *J. Phys. Chem. C* **121**(3), 1552–1561 (2017).

<sup>15</sup>B. Uhler, M. V. Ivanov, D. Kokkin, N. Reilly, R. Rathore, and S. A. Reid, *J. Phys. Chem. C* **121**(29), 15580–15588 (2017).

<sup>16</sup>S. A. Reid, S. Nyambo, A. Kalume, B. Uhler, C. Karshenas, and L. Muzangwa, *J. Phys. Chem. A* **117**(47), 12429–12437 (2013).

<sup>17</sup>L. Muzangwa, S. Nyambo, B. Uhler, and S. A. Reid, *J. Chem. Phys.* **137**(18), 184307 (2012).

<sup>18</sup>T. G. Dietz, M. A. Duncan, M. G. Liverman, and R. E. Smalley, *J. Chem. Phys.* **73**(10), 4816–4821 (1980).

<sup>19</sup>M. J. Frisch *et al.*, GAUSSIAN 09, Revision A, Gaussian, Inc., 2009.

<sup>20</sup>W. Z. Wang, T. Sun, Y. Zhang, and Y. B. Wang, *J. Chem. Phys.* **143**(11), 114312 (2015).

<sup>21</sup>J. P. Perdew, M. Emzerhof, and K. Burke, *J. Chem. Phys.* **105**(22), 9982–9985 (1996).

<sup>22</sup>C. Adamo and V. Barone, *Chem. Phys. Lett.* **314**(1-2), 152–157 (1999).

<sup>23</sup>S. Grimme, J. Antony, S. Ehrlich, and H. Krieg, *J. Chem. Phys.* **132**(15), 154104 (2010).

<sup>24</sup>A. J. Cohen, P. Mori-Sanchez, and W. T. Yang, *Chem. Rev.* **112**(1), 289–320 (2012).

<sup>25</sup>D. Kokkin, M. V. Ivanov, J. Loman, J.-Z. Cai, R. Rathore, and S. A. Reid, *J. Phys. Chem. Lett.* **9**(8), 2058–2061 (2018).

<sup>26</sup>M. R. Talipov, A. Boddada, Q. K. Timerghazin, and R. Rathore, *J. Phys. Chem. C* **118**(37), 21400–21408 (2014).

<sup>27</sup>M. Renz, K. Theilacker, C. Lambert, and M. Kaupp, *J. Am. Chem. Soc.* **131**(44), 16292–16302 (2009).

<sup>28</sup>M. Renz, M. Kess, M. Diedenhofen, A. Klamt, and M. Kaupp, *J. Chem. Theory Comput.* **8**(11), 4189–4203 (2012).

<sup>29</sup>C. Adamo and V. Barone, *Chem. Phys. Lett.* **274**(1-3), 242–250 (1997).

<sup>30</sup>F. Weigend, *Phys. Chem. Chem. Phys.* **8**(9), 1057–1065 (2006).

<sup>31</sup>F. Weigend and R. Ahlrichs, *Phys. Chem. Chem. Phys.* **7**(18), 3297–3305 (2005).

<sup>32</sup>J. A. Frey, C. Holzer, W. Klopper, and S. Leutwyler, *Chem. Rev.* **116**(9), 5614–5641 (2016).

<sup>33</sup>J. Rezac, D. Nachtigallova, F. Mazzoni, M. Pasquini, G. Pietraperzia, M. Becucci, K. Muller-Dethlefs, and P. Hobza, *Chem.–Eur. J.* **21**(18), 6740–6746 (2015).

<sup>34</sup>M. R. Talipov, M. V. Ivanov, S. A. Reid, and R. Rathore, *J. Phys. Chem. Lett.* **7**(15), 2915–2920 (2016).